Printed Loop Antenna With a U-Shaped Tuning Element for Hepta-Band Laptop Applications

Chien-Wen Chiu, *Member, IEEE*, and Yu-Jen Chi, *Student Member, IEEE*

***Abstract*—A simple printed-loop antenna with wideband characteristics is presented for laptop computer applications. The proposed rectangular loop pattern generates four resonant modes below 4 GHz. The excited modes, two unbalance and two balance, are analyzed and discussed. A novel U-shaped tuning element printed on the back side of the circuit board adjusts the resonant modes to cover GSM850/GSM900/DCS/PCS/UMTS/WLAN and WiMAX bands. Using HFSS software, this study conducted a simulation to optimize the antenna design and fabricate a practical structure to investigate its performance and characteristics. This study also measures various antenna parameters to validate the proposed antenna.**

***Index Terms*—Broadband antenna, mobile phone antenna, multiband antenna, portable device applications, printed loop antenna.**

I. Introduction

WITH the rapid progress in wireless communication, wireless networking has become a basic but important function for laptop computers. Besides the widely-used wireless local area network (WLAN) standard, the 3.5 G mobile communication system has become extremely popular. The 3.5 G system is based on the high speed downlink package access (HSDPA) protocol, allowing people to access the internet via cellular communication systems. In addition, worldwide interoperability for microwave access (WiMAX) technology, which provides wireless data transmission in a variety of ways, is an alternative for wider coverage than WLAN. To date, only a few internal antennas have been proposed for laptop computers [1]–[8], and even fewer of them can simultaneously cover all of the following communication standards: GSM850/900 (824–960 MHz), DCS (1710–1880 MHz), PCS (1850–1990 MHz), UMTS (1920–2170 MHz), WLAN + Bluetooth (2400–2484 MHz), and WiMAX (2500–2690 MHz).

Printed loop antennas have been widely used in laptop computers and mobile phones. Since laptop computers started out as computers and not as personal communication devices, antennas were not considered in the early development stage. As a result, the space allocated for antenna design is usually quite small and narrow. When an internal antenna is embedded into the top edge of an LCD panel, its geometrical configuration must be thin or rectangular, with a long length to width ratio, i.e., the practical antenna profile must be nearly planar: thin but long. In the past decade, researchers have proposed some practical antenna designs for laptop applications, some in the WLAN bands and some in the WWAN bands [1]–[5]. Recently, Wong *et al.*, demonstrated a printed monopole slot antenna can be attractive for multiband laptop computer applications. The proposed monopole slot antenna can achieve small size (60 mm $\times$ 12 mm) [6], [7]. To achieve low prices, a uniplanar inverted-F antenna was proposed for the above application. The uniplanar PIFA which is printed only on a single surface is easier to fabricate [8]. On the other hand, mobile phones, started out as a communication device, are typically equipped with printed antennas, which are planar, easy to fabricate and less expensive [9]–[11]. Therefore, some recent studies have proposed printed loop antennas mounted on top of the handset printed circuit board for mobile phone applications. These antennas can generate operating bands covering both GSM850/900 and DCS/PCS/UMTS standards, and are very promising designs [12], [13].

This paper presents a simple printed-loop antenna with wideband characteristics for laptop applications. The proposed antenna can be easily implemented in a printed circuit board and mounted on the LCD panel of a mini-laptop computer. Its rectangular loop pattern can generate four resonant modes below 4 GHz, two unbalance and two balance modes. The proposed design uses a grounded U-shaped tuning element printed on the back side of the circuit board to adjust the resonant modes to cover GSM850/GSM900/DCS/PCS/UMTS/WLAN and WiMAX bands. The proposed antenna covers sufficient bands to support the desired operation bands. This planar antenna requires only a volume of $65 \times 10 \times 0.8\ \mathrm{mm}^3$. To optimize the design of this antenna, this paper performs HFSS simulations and fabricates a practical structure to verify the simulation results. The actual measured antenna parameters are presented to validate the proposed antenna. In contrast to some recent proposed laptop antennas [6]–[8], the current one is double-sided and has slight larger size. However, it covers not only WWAN band but also WLAN and WiMAX bands.

II. Antenna Design

Fig. 1(a) shows the configuration of the proposed antenna. The antenna is printed on a FR4 substrate with a thickness of 0.8 mm and a relative permittivity of 4.4. The antenna is mounted on the top-right corner of a vertical ground plane (of size $200 \times 160\ \mathrm{mm}^2$), which is the supporting metal frame of a LCD panel. Because the antenna is coated on the double-sided PCB, it measures only $65 \times 10 \times 0.8\ \mathrm{mm}^3$. Fig. 1(b) and (c) show the antenna patterns on the front and back sides of the printed circuit board.

Manuscript received June 23, 2009; revised May 11, 2010; accepted May 20, 2010. Date of publication August 30, 2010; date of current version November 03, 2010. This work was supported in part by the Taiwan National Science Committee under Grant NSC-96-2221-E-197-001.

The authors are with the Department of Electronic Engineering, National Ilan University, Ilan, Taiwan, R.O.C. (e-mail: alexchiu@niu.edu.tw).

Color versions of one or more of the figures in this paper are available online at http://ieeexplore.ieee.org.

Digital Object Identifier 10.1109/TAP.2010.2071343

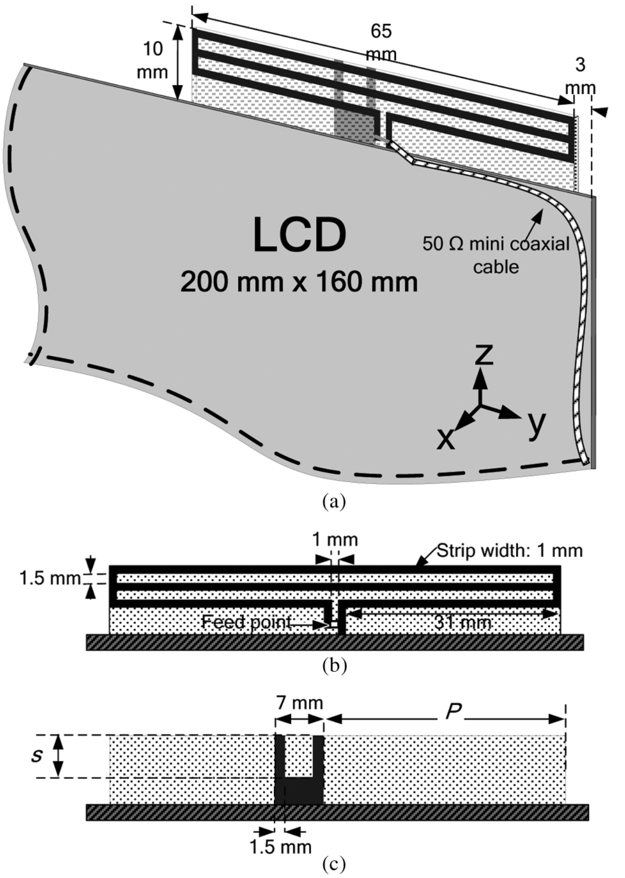

Fig. 1. Geometry of the proposed antenna, (a) 3D view, (b) plan view of the front-side, and (c) plan view of the back-side.

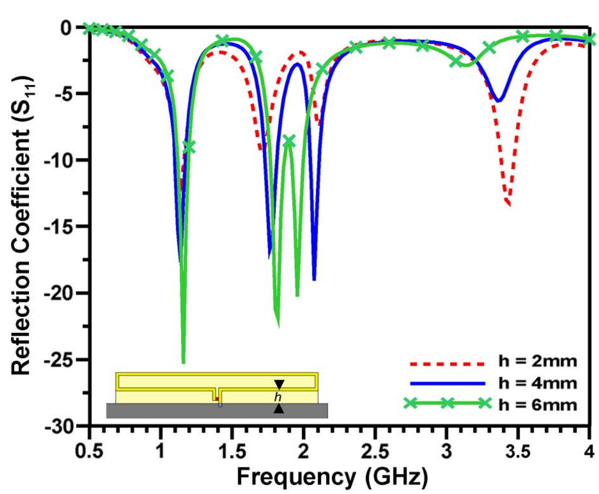

Fig. 2. Simulation results as a function of different heights.

The U-shape on the back side is a tuning element, which is affixed to the ground plane. The antenna is fed by a 50 Ω mini coaxial cable. The center conductor of the cable launches the signal into the strip end on the left hand-side of the loop pattern. The outer conductor of the cable is connected to the right hand-side of the loop strip that terminates to the ground plane.

The proposed antenna has a one-wavelength rectangular loop design. The final design originates from a simple rectangular loop pattern that is illustrated in Fig. 2. The distance between the loop pattern and the vertical ground plane is defined as height h.

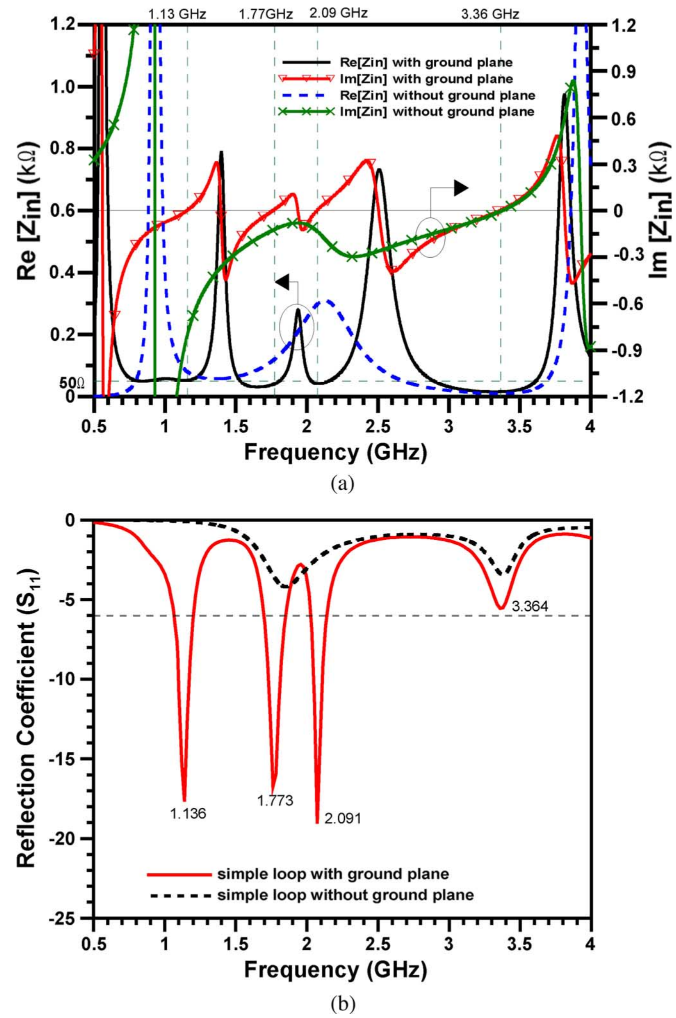

Fig. 3. Simulation results for the simple loop pattern.

Since the loop antenna structure is a one-wavelength resonator, the perimeter of the initial loop antenna can be determined by the resonant frequency of the lowest loop-mode [10]–[12]. The total length l of the simple loop pattern can simply be calculated. The calculated wavelength is 150 mm at 2 GHz. However, because the loop pattern is printed on the edge of the thin circuit board near the ground plane, the conductor plane and the substrate may influence the electromagnetic field. After some simulations with multiband consideration, the initial-guess perimeter for the loop is designed to around $65+10+65+10 = 150\ \mathrm{mm}$. Fig. 2 shows the influence of varying the height h on the reflection coefficient, suggesting that the distance between the bottom of the loop pattern and the vertical ground plane can be used to adjust the input impedance. The best impedance matching occurs at a height $\mathrm{h} = 6\ \mathrm{mm}$, but the height is finally adjusted to 4 mm in taking the overall design consideration.

Fig. 3(a) shows the real and imaginary parts of the input impedance, while (b) shows the simulated reflection coefficient for the simple loop antenna with and without the vertical ground plane. The loop antenna is symmetric when there is no system ground plane, and this loop antenna can generate traditional loop modes. The first resonant mode at 0.95 GHz (half-wavelength) has very high values of resistance and reactance (the so-called parallel type, referred to as anti-resonance) [14]. It does not match

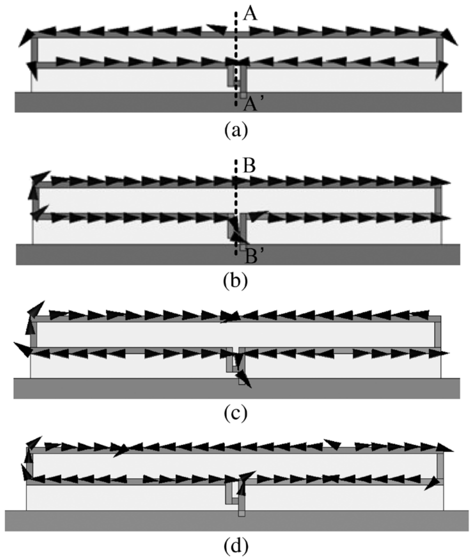

Fig. 4. Simulated vector current distributions. (a) 1.136 GHz; (b) 1.773 GHz; (c) 2.091 GHz; (d) 3.364 GHz.

a 50 Ω transmission line, and therefore does not generate resonance, as Fig. 3(b) shows. The second resonant mode, generated at 1.9 GHz, is a one-wavelength loop mode since the wavelength is about 150 mm. Fig. 3(a) shows that the antenna has smaller values of resistance and reactance (the so-called series type, resonant-mode) [14]. The input impedance allows the matching of 50 Ω transmission lines, and thus the generation of resonance.

When the system ground plane is added, the strip end in the right-hand side terminates at the ground plane and the strip end in the left-hand side is fed by a coaxial cable, as Fig. 1 shows. The outer conductor of the coaxial cable is also connected to the grounded strip. The resulting antenna system has a symmetric loop pattern, but an unbalanced feeding scheme. The unbalance mode and balance mode can be simultaneously excited on this antenna system. Therefore, the antenna system generates four resonant modes (series type) below 4 GHz, as Fig. 3(a) and (b) show. The presence of the conducting ground plane shifts the resonant frequencies. The first resonant mode at 1.136 GHz is an unbalance mode, and the mode at 2.091 GHz is its higher mode. The second resonant mode, at 1.773 GHz, is a balance mode, and the mode at 3.364 GHz is its higher mode.

To demonstrate that the unbalance mode creates the resonances at 1.136 GHz and 2.091 GHz and that the self-balanced loop mode creates the resonance at 1.773 GHz and 3.364 GHz, Fig. 4 shows the vector current distributions and Fig. 5 shows the surface current densities at 1.136, 1.773, 2.091 and 3.364 GHz, respectively. These results are simulated by HFSS, a commercial electromagnetic simulation tool. The currents shown in Fig. 4(a) and (c) are equal in amplitude, but in the opposite direction since the loop pattern is symmetric from side to side with respect to the line AA'. This behavior and the current density in Fig. 5(a) and (c) imply that the feeding scheme excites the unbalance modes. The current shown in Fig. 4(b) and (d) exhibits a differential behavior in the feeding port. In this case, the currents are equal in amplitude and in the same direction with respect to the line BB'. Obviously, they are one- and two-wavelength loop modes. The balance modes are excited when the electric length of the loop pattern is close to one- or two-wavelength.

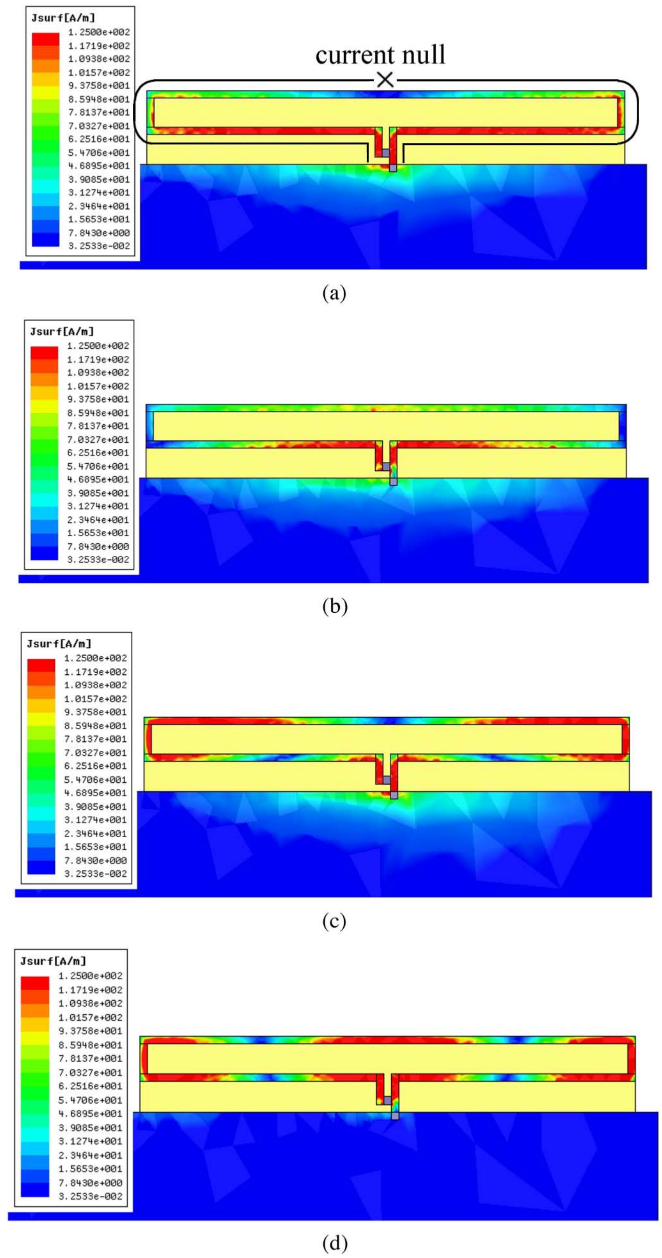

Fig. 5. Simulated surface current density of the loop antenna. (a) 1.136 GHz; (b) 1.773 GHz; (c) 2.091 GHz; (d) 3.364 GHz.

On the other hand, the currents along the y-direction in Fig. 4(b) are in the same direction at 1.773 GHz. This characteristics show that the antenna at this mode can also be viewed as a folded dipole [15]. If the effect of ground plane is considered, the half length of the perimeter of the loop (75 mm) is close to the 0.5 wavelength of a dipole antenna at 1.773 GHz. Theoretically, the impedance of a folded dipole is about four times greater than that of an isolated dipole [15]. However, in the present case, there is a substrate and a nearby ground plate below the feeding strip. The upper strip is printed near the edge of substrate, which is more distant from the ground plate than the feeding strip. The current density in Fig. 5(b) on the lower strip is stronger than that on the upper strip. As a result, the current ratio becomes smaller, e.g., $\mathrm{I_2/I_1} = 0.65$, at the resonating frequency 1.773 GHz by HFSS simulation, where

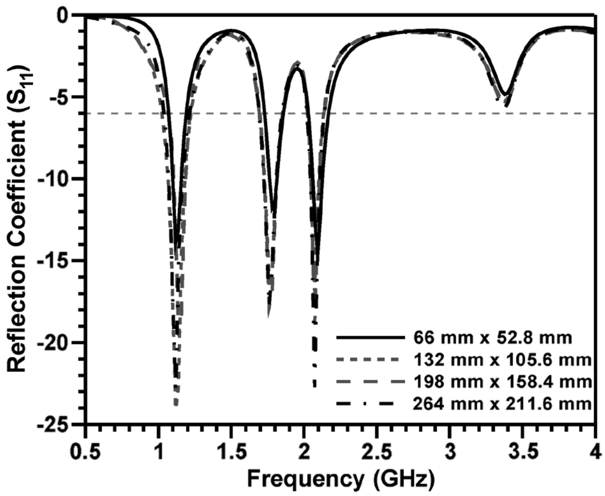

Fig. 6. Simulated reflection coefficient with the size of LCD ground plane as a parameter ($\lambda = 264\ \mathrm{mm}$ at 1.136 GHz).

I_1 and I_2 are the total currents on the lower and upper strips, respectively. The step-up impedance ratio is much smaller than that predicted by traditional folded dipole.

Finally, some explanations are necessary to account for how the vertical ground plane affects excitations of the unbalance modes and matching of the input impedance. The loop pattern which terminates to the ground plane is fed by an unbalanced feeding port. Due to the presence of the ground plane, the feeding scheme can have not only the balanced but also unbalanced excitation. The half-wavelength mode of a single loop antenna, which is an anti-resonance mode, can be supported by the unbalanced excitation. Since there is a current null for the surface current shown in Fig. 5(a) in this mode, the loop can be viewed as consisting of two arms. The currents on the two arms of the loop are of the same phase. As a result, the arms behave like two parallel bent monopoles mounted on the vertical ground plane. Since the length of one arm is around 70 mm $(3 + 31 + 5 + 31)$, the resonant frequency of the monopole-like mode is calculated to be about 1.07 GHz (wavelength 280 mm), which corresponds to the resonant frequency of the first resonance mode shown in Fig. 3(b). The resonant frequency of the first unbalance mode is mainly determined by the arm length of the loop pattern but also influenced by the ground plane. The monopole-like mode can also be verified by the radiation patterns discussed in Section IV, where E_Θ in the x-y plane is basically omni-directional.

The large ground plane, which is larger than half a wavelength at the first resonance mode 1.136 GHz, is more like a reflector, not an efficient radiator [3]. Fig. 6 shows the simulated reflection coefficient with the size of LCD ground plane as a parameter. The large ground plane shown in Fig. 1(a) is located nearly on the same plane with the loop. The finding shows that changing the size of the ground plane has no significant influence on the resonance frequency if only the ground plane size is larger than 0.25λ (66 mm). If the ground plane size is less than a quarter-wavelength, the ground plane has significant influence on the impedance matching at the resonance modes. When the size of the ground plane is reduced from one-wavelength to quarter-wavelength, the bandwidth of the first resonance mode gradually decreases from 160 MHz to 110 MHz.

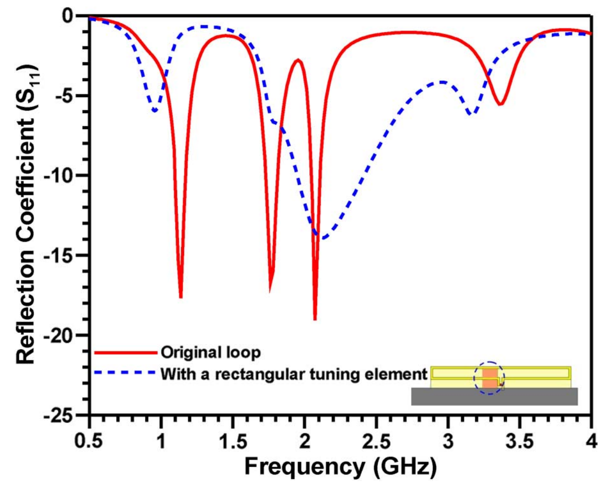

Fig. 7. Simulated results after adding a grounded-rectangular tuning element.

III. Bandwidth Enhancement by a Matching Element

Although the proposed antenna can generate two resonant modes at 1.773 and 2.091 GHz, the bandwidth achieved is not wide enough to cover UMTS, WiFi, and WiMAX operations for the antenna's upper band. Therefore, this study applied another bandwidth-enhancement technique to achieve better wideband performance. To achieve better bandwidth performance, a parasitic load shown in Fig. 1(c), a grounded tuning element, is used to lower the resonant frequency at 3.364 GHz. The position of this short-circuited element can be decided by investigating the surface current distribution. Since the currents shown in Fig. 5(b) and (d) are strong at the feeding center of the loop antenna, placing the tuning element near this area will dramatically influence the resonant modes. The tuning element, coupled with the antenna, can effectively decrease the fourth-order resonant mode at 3.364 GHz resulting in lower resonant frequencies.

Fig. 7 shows the effect of adding a grounded-rectangular tuning element to the back of the printed circuit board. Adding this tuning element broadens the bandwidth from 1.75 GHz to 2.70 GHz. However, the addition of this tuning element may affect the impedance matching at the GSM900 band since the maximum electric field distributions at 1 GHz are located in the center of the loop pattern. In this works, the radiation field that comes from the ground plane is small since the area of the ground plane is large and the induced current on the ground plane is small. The radiation resistance of the input impedance decreases when the tuning element is short-circuited to the ground plane. As a result, the impedance matching deteriorates and the reflection coefficient fails to reach -10 dB. The U-shaped tuning element in Fig. 1(c) is preferred to a rectangular one since it can decrease the impedance matching effect at 1 GHz. Fig. 8 shows a parametric study of the concave depth s on the rectangular tuning element. The widest bandwidth at the GSM band occurs when $s = 8\ \mathrm{mm}$. Impedance matching also improves in the higher bands as the depth s increases. Finally, Fig. 8 shows that when the concave depth is 6 mm, the reflection coefficient is close to -10 dB, which meets the requirements and specifications of WLAN and WiMAX applications.

Although introducing a U-shaped concavity to the tuning element helps it match the input impedance at the GSM band, the resonant frequency at the GSM band is a little higher than the

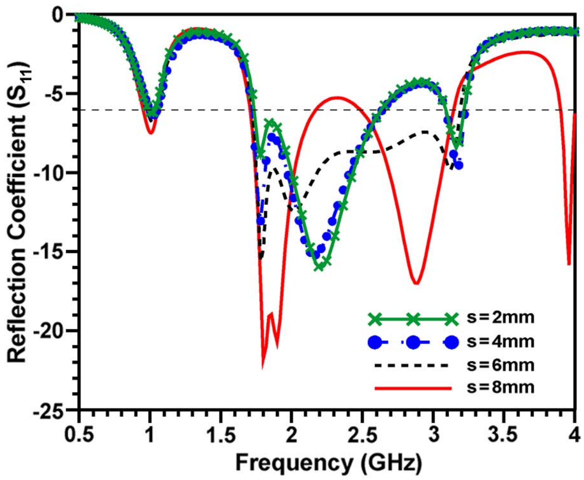

Fig. 8. Simulated results when a concave is introduced to the rectangular tuning element.

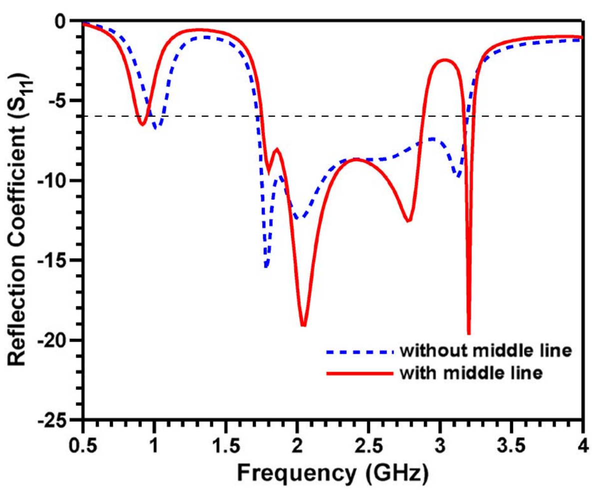

Fig. 9. Frequency shifting down as a middle line has been added.

desired operating frequency. Therefore, a horizontal strip line is inserted into the loop pattern to increase the electric length, as Fig. 1 shows. Fig. 9 shows the simulated results with and without inserting the middle line. This figure demonstrates that inserting a middle strip line shifts the resonance to a lower band. However, it also reduces the impedance bandwidth in the higher band from 1500 MHz (1.7 GHz $\sim$ 3.2 GHz) to 1100 MHz (1.7 GHz $\sim$ 2.8 GHz). In addition, the input impedances are $61.6 + \text{j}6.2\ (\Omega)$ and $39.91 - \text{j}1.66\ (\Omega)$ at the second resonance mode for the folded dipole with and without the middle line, respectively. The step-up impedance ratio between the two cases (three lines and two lines) is simulated to be 1.6. The value is different from the traditional prediction of $9/4 = 2.25$ due to the substrate and the ground plane effects.

The location where an antenna is attached to on the supporting metal frame is not unique. The antenna can be mounted on the vertical or horizontal edge of an LCD display. According to the location and orientation evaluation at IBM, bandwidths will be wider if the antenna is placed at the top edge of a large ground plane [16]. Fig. 10 shows the location effect of the antenna on the impedance matching. Here, d is the distance between the antenna and the top-right edge of the LCD panel. The size of the LCD

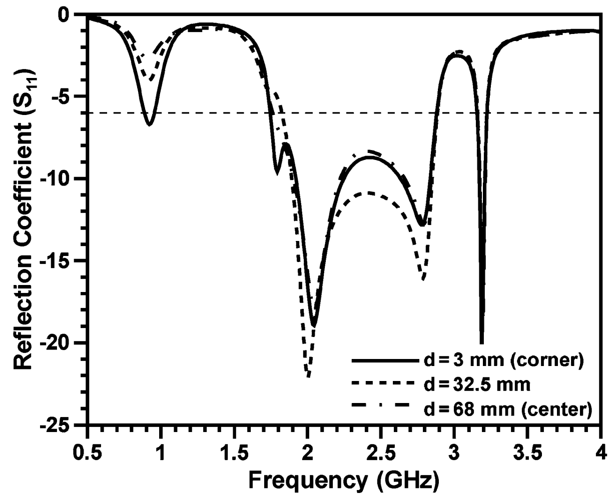

Fig. 10. Simulated reflection coefficient as a function of the distance d.

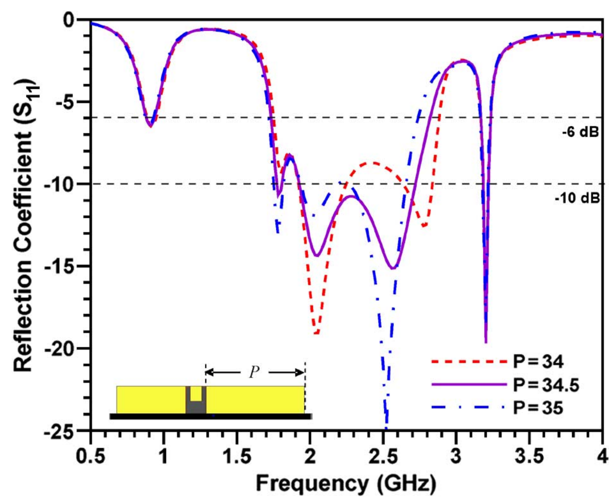

Fig. 11. Effect of varying position P from 34 mm to 35 mm.

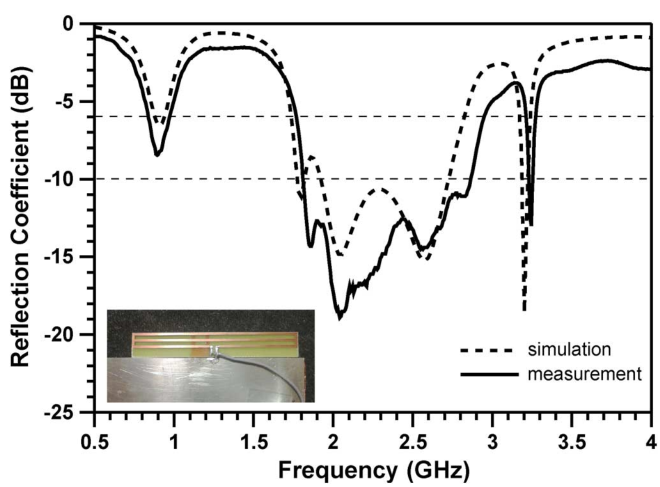

Fig. 12. Measured and simulated results for the proposed antenna.

panel which measures 200 mm $\times$ 160 mm is different from the system ground plane of a mobile phone. The figure shows that the resonant frequency remains almost unchanged but the input impedance will be influenced if the antenna is moved along the top edge. Moving the antenna along the top edge has significant

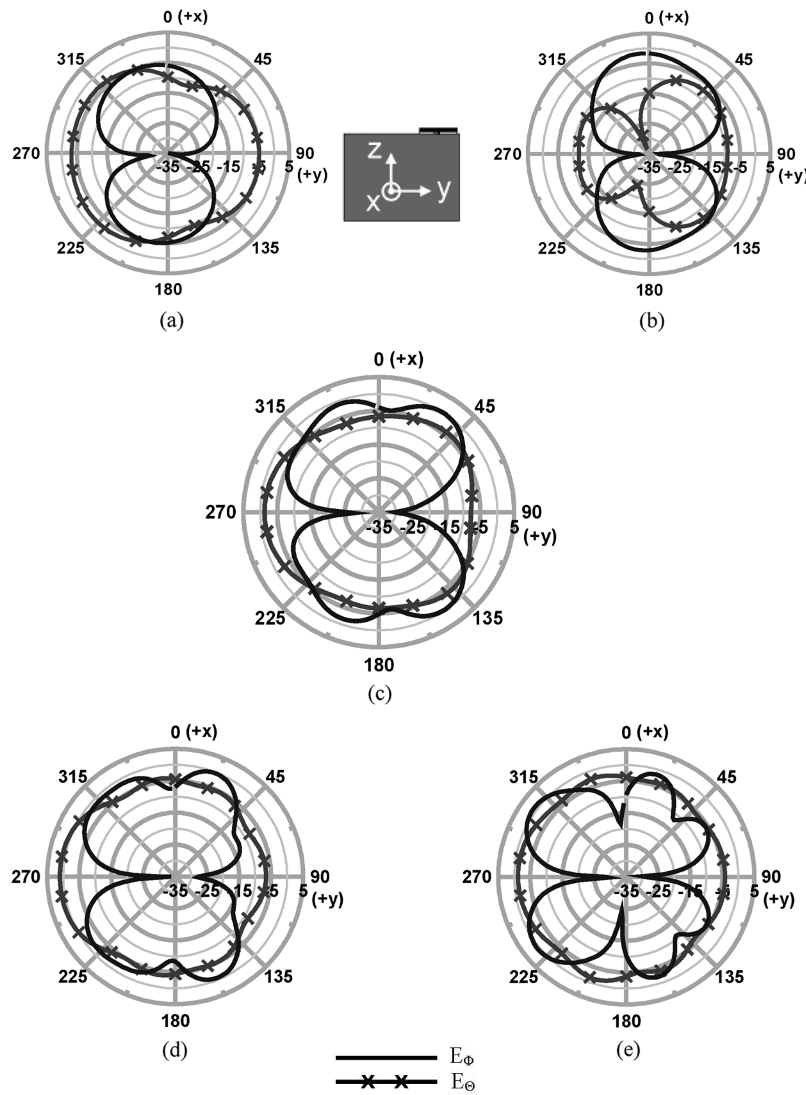

Fig. 13. Measured radiation patterns on the horizontal plane. (a) 900 MHz; (b) 1.80 GHz; (c) 2.10 GHz; (d) 2.45 GHz; (e) 2.70 GHz.

effects on the bandwidth, especially in the low GSM band. It indicates that the bandwidth is wider if the antenna is placed near the top-right corner, i.e., $d = 3$. The current distributions shown in Fig. 5(a) have no significant difference on the ground plane but have some change on the loop pattern when the antenna placed near the right corner is compared with that at the top-center of the ground plane. The study finds that better impedance matching is achieved when the loop is placed near the top-right corner than when it is placed at the top center.

Finally, Fig. 11 shows the influence of the position of the U-shaped tuning element on antenna performance. The simulated reflection coefficient for position P, which varies from 34 mm to 35 mm, shows that the fourth-order resonant frequency can be shifted to the lower band and a wide band operation can be obtained when P is 34.5 mm. The position is rather sensitive especially when the tuning element is nearby the feeding port. Since using the coupled tuning element introduces too many loaded effects, the U-shaped tuning element is better than a rectangular shape for obtaining a good impedance match to 50 Ω at high frequencies.

IV. Measured Results and Discussion

This study constructed a practical antenna based on the structure shown in Fig. 1. It was tested and measurements were taken using a Network Analyzer E5071B. The measured results were then compared with the simulation results produced by HFSS software. Fig. 12 shows both the experimental results and the simulation results. The solid line in this figure shows the measured results, while the dashed line shows the simulated results. These results exhibit good overall agreement, except for some loss caused by a 200 mm mini-coaxial cable. The bandwidth achieved with a reflection coefficient better than -6 dB is 140 MHz (820–960 MHz) in the GSM band and 1190 MHz (1710–2900 MHz) in the DCS/PCS/UMTS bands. The bandwidth with a reflection coefficient better than -10 dB is sufficient for WLAN and WiMAX applications.

The radiation pattern and gain were measured in an anechoic chamber using a Satimo system—SG24 in Taiwan. Fig. 13 shows the measured radiation patterns of the proposed antenna on the horizontal plane (x-y plane). Monopole-like patterns are evident at the unbalance modes, as Fig. 13(a) and (c) shows. A fairly omni-

TABLE I
MEASURED PEAK GAIN, TWO-DIMENSIONAL AVERAGE GAIN, AND RADIATION EFFICIENCY

Freq. (GHz)	0.9	1.80	2.10	2.45	2.70
Peak Gain (dBi)	1.12	3.13	2.26	1.82	3.21
Avg. Gain (dBi)	-3.21	-4.87	-1.24	-0.83	-0.79
Efficiency (%)	46.4	60.5	80.6	74.8	67.6

directional pattern can be observed for E_Θ, except for 1.8 GHz although the measured E_Θ and E_Θ patterns for the folded-dipole mode at 1.8 GHz are somewhat directional and some variations and nulls can be found in the E_Θ patterns. The omni-directional feature is perfectly suitable for laptop computers.

Table I lists the measured peak gain, two-dimensional average gain in the horizontal plane, and three-dimensional radiation efficiency of the proposed antenna. The antenna gain is approximately 1.12–3.21 dBi. Note that the measured gain results include the loss of a 200 mm mini-coaxial cable. The mini-coaxial cable (I-PEX) used for laptop or netbook computers has a very small diameter, around 1.1 mm, for routing through hinges. Therefore, the cable has more than 3 dB/m loss at the operating bands. This loss effect reduces the antenna gain by about 0.6 dB. Nonetheless, the obtained antenna gain and radiation efficiency are still good for practical applications in laptop computers despite cable loss.

V. CONCLUSION

This paper proposes a simple printed loop antenna with multiband characteristics that integrate WWAN and WLAN/WiMAX systems. The proposed system consists of a loop pattern and a novel U-shaped tuning element on each side of a printed circuit board. The loop pattern generates four resonating modes below 4 GHz, while the grounded U-shaped tuning element broadens the impedance bandwidth. To validate the proposed design, this study also presents parameter measurements for the reflection coefficient, radiation patterns, antenna gain, and radiation efficiency. The proposed two-dimensional planar-type antenna is compact, wideband, and easy to fabricate, making it very suitable for today's popular small netbook computers.

ACKNOWLEDGMENT

The authors are grateful to the National Center for High-performance Computing for computer time and the use of their facilities. They would also like to thank Prof. S. M. Deng at MCU for helpful discussions and the reviewers for their comments and suggestions.

REFERENCES

[1] K. L. Wong, L. C. Chou, and C. M. Su, "Dual-band flat-plate antenna with a shorted parasitic element for laptop applications," *IEEE Trans. Antennas Propag.*, vol. 53, pp. 539–544, Jan. 2005.

[2] D. Liu and B. Gaucher, "A quadband antenna for laptop applications," in *Proc. IEEE Antennas and Propagation Society Int. Symp.*, Hawaii, Jun. 2007, pp. 128–131.

[3] C. H. Kuo, K. L. Wong, and F. S. Chang, "Internal GSM/DCS dual-band open-loop antenna for laptop application," *Microw. Opt. Technol. Lett.*, vol. 49, pp. 680–684, Mar. 2007.

[4] C. Zhang, S. Yang, S. Lee, S. E. Ghazaly, A. E. Fathy, H. K. Pan, and V. K. Nair, "A low profile twin-PIFA laptop reconfigurable multi-band antenna for switchable and fixed services wireless applications," in *Proc. IEEE Antennas and Propagation Society Int. Symp.*, Hawaii, Jun. 2007, pp. 1209–1212.

[5] C. W. Chiu, Y. J. Chi, and S. M. Deng, "An internal multiband antenna for WLAN and WWAN applications," *Microw. Opt. Technol. Lett.*, vol. 51, pp. 1803–1807, Aug. 2009.

[6] K. L. Wong and L. C. Lee, "Multiband printed monopole slot antenna for WWAN operation in the laptop computer," *IEEE Trans. Antennas Propag.*, vol. 57, pp. 324–330, Feb. 2009.

[7] K. L. Wong and F. H. Chu, "Internal planar WWAN laptop computer antenna using monopole slot elements," *Microw. Opt. Technol. Lett.*, vol. 51, pp. 1274–1279, May 2009.

[8] K. L. Wong and S. J. Liao, "Uniplanar coupled-fed printed PIFA for WWAN operation in the laptop computer," *Microw. Opt. Technol. Lett.*, vol. 51, pp. 549–554, Feb. 2009.

[9] T. A. Denidni, H. J. Lee, Y. S. Lim, and Q. Rao, "Wide-band high-efficiency printed loop antenna design for wireless communication systems," *IEEE Trans. Vehicular Tech.*, vol. 54, pp. 873–878, May 2005.

[10] Y. W. Chi and K. L. Wong, "Internal compact dual-band printed loop antenna for mobile phone application," *IEEE Trans. Antennas Propag.*, vol. 55, pp. 1457–1462, May 2007.

[11] B. Jung, H. Rhyu, Y. J. Lee, F. J. Harackiewwicz, M. J. Park, and B. Lee, "Internal folded loop antenna with tuning notches for GSM/GPS/DCS/PCS mobile handset applications," *Microw. Opt. Technol. Lett.*, vol. 48, pp. 1501–1504, Aug. 2006.

[12] K. L. Wong and C. H. Huang, "Printed loop antenna with a perpendicular feed for penta-band mobile phone application," *IEEE Trans. Antennas Propag.*, vol. 56, pp. 2138–2141, Jul. 2008.

[13] Y. W. Chi and K. L. Wong, "Quarter-wavelength printed loop antenna with an internal printed matching circuit for GSM/DCS/PSC/UMTS operation in the mobile phone," *IEEE Trans. Antennas Propag.*, vol. 57, pp. 2541–2547, Sep. 2009.

[14] K. D. Katsibas, C. A. Balanis, P. A. Tirkas, and C. R. Birtcher, "Folded loop antenna for mobile hand-held units," *IEEE Trans. Antennas Propag.*, vol. 46, pp. 260–266, Feb. 1998.

[15] C. A. Balanis*, Antenna Theory, Analysis and Design*, 2nd ed. New York: Wiley, 1997, pp. 458–462.

[16] Z. N. Chen*, Antennas for Portable Devices*. West Sussex, U.K.: Wiley, 2007, pp. 122–124.

Chien-Wen Chiu (M'98) was born in Maoli, Taiwan, R.O.C., in 1962. He received the B. S. degree from National Taiwan Normal University, Taipei, in 1984, and the M.S. and Ph.D. degrees in electrical engineering from National Taiwan University, Taipei, in 1990 and 1996, respectively.

From 1990 to 1991, he was a member of the Computer and Communication Research Laboratory, Industrial Technology Research Institute, where his primary research focus was the development of the DECT system. From 1991 to 1997, he was with the Department of Electronic Engineering, Jinwen University of Science and Technology, where he was a Lecturer until 1996 when he became an Associate Professor. From 1997 to 2003, he was with the Department of Electronic Engineering, Minghsin University of Science and Technology. In 2003, he joined the Department of Electronic Engineering, National Ilan University, where he is currently an Associate Professor. He is presently the Chairman of the Bachelor Program for the College of Electrical Engineering and Computer Science. His research interests include mobile antenna design, electromagnetic computations, electromagnetic compatibility, and RF ID antenna design.

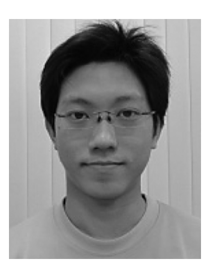

Yu-Jen Chi (S'98) was born in Taipei, Taiwan, R.O.C., in 1985. He received the B.S. and M.S. degrees in electronic engineering from National Ilan University, I-Lan, Taiwan, R.O.C., in 2007 and 2009, respectively. He is currently working toward the Ph.D. degree at National Chiao Tung University, Hsinchu, Taiwan, R.O.C.

His main research interests are in multiband antennas for mobile devices, CRLH leaky wave antenna, and metamaterials.

Mr. Chi received the Best Poster Award from the International Workshop on Antenna Technology (iWAT 2009).